JOURNAL OF VIROLOGY, June 1995, p. 3605–3614 Vol. 69, No. 6
0022-538X/95/$04.00+0

RNA-Protein Interactions Directed by the 3′ End of Human Rhinovirus Genomic RNA

STEPHEN TODD, JOSEPH H. C. NGUYEN, AND BERT L. SEMLER*

Department of Microbiology and Molecular Genetics, College of Medicine, University of California, Irvine, California 92717

Received 19 September 1994/Accepted 26 February 1995

The replication of a picornavirus genomic RNA is a template-specific process involving the recognition of viral RNAs as target replication templates for the membrane-bound viral replication initiation complex. The virus-encoded RNA-dependent RNA polymerase, $3D^{pol}$, is a major component of the replication complex; however, when supplied with a primed template, $3D^{pol}$ is capable of copying polyadenylated RNAs which are not of viral origin. Therefore, there must be some other molecular mechanism to direct the specific assembly of the replication initiation complex at the 3′ end of viral genomic RNAs, presumably involving *cis*-acting binding determinants within the 3′ noncoding region (3′ NCR). This report describes the use of an in vitro UV cross-linking assay to identify proteins which interact with the 3′ NCR of human rhinovirus 14 RNA. A cellular protein(s) was identified in cytoplasmic extracts from human rhinovirus 14-infected cells which had a marked binding preference for RNAs containing the rhinovirus 3′ NCR sequence. This protein(s) showed reduced cross-linking efficiency for a 3′ NCR with an engineered deletion. Virus recovered from RNA transfections with in vitro transcribed RNA containing the same 3′ NCR deletion demonstrated a defective replication phenotype in vivo. Cross-linking experiments with RNAs containing the poliovirus 3′ NCR and cytoplasmic extracts from poliovirus-infected cells produced an RNA-protein complex with indistinguishable electrophoretic properties, suggesting that the appearance of the cellular protein(s) may be a common phenomenon of picornavirus infection. We suggest that the observed cellular protein(s) is sequestered or modified as a result of rhinovirus or poliovirus infection and is utilized in viral RNA replication, perhaps by binding to the 3′ NCR as a prerequisite for replication complex assembly at the 3′ end of the viral genomic RNA.

The replication of an RNA genome by a positive-strand RNA virus, such as a picornavirus, is a consequence of specific RNA-RNA, RNA-protein, and protein-protein interactions. RNA-RNA interactions manifest themselves both in intermolecular forms, such as base complementarity in the replicative-intermediate (7, 34) and replicative-form (4, 7, 34) viral intermediate RNAs, and in intramolecular RNA secondary- and tertiary-structure motifs, such as the pseudoknot structure proposed in the 3′ noncoding region (3′ NCR) of poliovirus genomic RNA (30, 37). The role of protein-protein interactions involved in positive-strand RNA virus replication has not been well defined; the study of these interactions in the picornavirus system is complicated by the tight membrane association of virtually all virus-associated activities (8, 9). The dissection of membranous viral replication complexes has proven difficult. The main focus of this study, RNA-protein interactions, is perhaps the most crucial element of the specific recognition of viral RNAs as replication templates for the viral replication machinery. Specific RNA-protein interactions may function as the nucleation point for the assembly of a competent viral replication initiation complex or may be the final recognition event to direct a preassembled replication complex onto its target viral RNA template.

In an effort to better understand the molecular mechanism of picornavirus RNA replication initiation at the level of RNA-protein interactions, experiments were undertaken to investigate the specific recognition determinants within the rhinovirus genomic RNA which are responsible for the amplification of the viral RNA by the virus-encoded RNA polymerase. The rhinoviruses are small naked icosahedral viruses with a single positive-strand (mRNA sense) RNA genome. The rhinoviruses differ slightly from the prototypic picornavirus, poliovirus (PV), an enterovirus (21), mainly in their smaller genome size and in the smaller size of their mature gene products. The genomic organization and function of the viral gene products of these two picornaviruses are apparently identical. Human rhinovirus 14 (HRV14) has a genome length of 7,212 nucleotides (nt), including a 5′ NCR of 629 nt and a 3′ NCR of 44 nt (10). All HRV14 proteins appear to be proteolytically processed by a similar if not identical cascade to that for PV gene products. Presumably as a result of adaptation to the nasal-pharyngeal cavities of humans, rhinovirus has an optimal growth temperature of 33 to 34°C (compared with 37°C for PV). The smaller size of the HRV14 3′ NCR compared with that of PV RNA offers the potential advantage of minimizing the sequence and/or secondary-structure requirements involved in RNA-protein recognition, and it reduces the size of the region to be genetically manipulated for such studies. The availability of a full-length infectious cDNA clone of HRV14 (31) facilitates the use of rhinovirus for both in vitro biochemical analyses and in vivo genetic manipulation.

In this study, we used a UV-cross-linking assay to investigate RNA-protein interactions at the 3′ end of a picornavirus genomic RNA. We report interaction with the HRV14 3′ NCR of a cellular protein, which appears to be sequestered or modified as the result of HRV14 infection. We further conclude that the appearance of this protein may be a general phenomenon of picornavirus infection in that the host factor(s) present in extracts from cells infected with either HRV14 or PV1 has binding preference for the 3′ NCRs of both viruses. A mutated HRV14 3′ NCR shows decreased binding of the host factor(s) in vitro, and rhinovirus bearing the same mutation demon-

* Corresponding author. Phone: (714) 824-7573. Fax: (714) 824-8598. Electronic mail address: BLSEMLER@UCI.EDU.

strates a defective replication phenotype in vivo. We postulate that this cellular factor may be utilized by HRV14 and PV1 in RNA replication, and perhaps its binding is a prerequisite for the formation of a virus-specific replication initiation complex on the picornavirus plus-strand template.

MATERIALS AND METHODS

Generation of a full-length, T7-based HRV14 cDNA construct. Plasmid pSP64(RV), originally obtained from Richard Colonno, contains an infectious cDNA copy of the HRV14 genome under control of an SP6 promoter. The resulting in vitro transcribed RNA has 21 additional nucleotides at its 5′ end which are not of viral origin (31). To increase the transfection efficiency of in vitro transcribed RNAs, the HRV14 cDNA was engineered into a T7-based transcription vector designed to produce an RNA with only two additional G nucleotides at the 5′ end. A fragment of pSP64(RV) corresponding to a portion of the HRV14 5′ noncoding region from the restriction sites *Fok*I (nt 24) to *Eco*RI (nt 343) was inserted into pGEM1 (Promega) between *Pvu*II (nt 98) and *Eco*RI (nt 52) by using the following synthetic oligonucleotides: HN1, 5′-ACGCG**TAATACGACTCACTATAG**-3′ (+); HN2, 5′-TAA**CCTATAGTGAG TCGTATTA**CGCGT-3′ (−); HN3, 5′-**G**TTAAAACAGCGGATGGGTATCC CA-3′ (+); and HN4, 5′-ATGGTGGGATACCCATCCGCTGTTT-3′ (−). The two pairs of complementary synthetic oligonucleotides (HN1/HN3 and HN2/HN4) were annealed and incubated with the above pSP64(RV) and pGEM1 fragments in the presence of T4 DNA ligase. The resulting DNA was transformed into competent *Escherichia coli* C600 cells, and colonies were screened for plasmid pT7RV5′. This plasmid contains a unique *Mlu*I site to replace the former pGEM1 *Pvu*II site (nt 98), a T7 promoter (bold) with a GG start, and the cDNA sequence corresponding to the 5′ end of HRV14 up to a *Fok*I half-site (nt 24). The subgenomic pT7RV5′ transcription vector was then digested with *Sna*BI (nt 258), which cuts within the subgenomic HRV14 cDNA sequence, and *Pst*I (nt 20), which digests pGEM1 in the polylinker sequence. The remaining ~7-kb HRV14 cDNA sequence from the unique *Sna*BI site (nt 258) to a *Pst*I site located just 3′ to the 3′ poly(A) tract encoded in pSP64(RV) was then cloned into the pT7RV5′ transcription vector background to yield pT7RV(FL), a full-length T7-based cDNA clone of HRV14 with only two nonviral nucleotides at the 5′ end of in vitro generated transcripts.

Construction of subgenomic HRV14 and PV1 transcription vectors. Subgenomic, T7-based transcription vectors were constructed from the full-length cDNA construct pT7RV(FL) described above. The plasmid was digested with *Mlu*I, which cuts at the engineered vector site (nt ~98), and *Hpa*I, which cuts in the HRV14 cDNA sequence at a location corresponding to sequences just upstream of the 3′ NCR (HRV14 nt 7169). The DNA fragment containing the cDNA sequence of the 3′ NCR and poly(A)$_n$ tract plus a *Pst*I linearization site (nt 7227 [HRV14]/nt 20 [pGEM1]) and vector sequence was incubated in the presence of T4 DNA ligase with the annealed synthetic oligonucleotides T7RV3′(+) (5′-CGCG**TAATACGACTCACTATAGG**TT-3′) and T7RV3′(−) (5′-AA**CCTATAGTGAGTCGTATTA**-3′) which contain (5′ to 3′) a *Mlu*I half-site, a T7 promoter (bold), and a *Hpa*I half-site. Following transformation and clone identification, the resulting transcription vector, pT7RV7168A+, was used to generate T7 transcripts with 5′-**G**GUUaac-, where the boldface **G** corresponds to the third-position nucleotide of the viral RNA stop codon (UA**G**) at the end of the 3D^{pol}-coding sequence. The 5′ end of the synthetic transcript therefore has the identical sequence to the viral genomic RNA in this region. Linearization of the vector with *Pst*I results in an RNA which terminates -A$_n$GG-3′ (where $n \approx$ 85 to 90) as a result of the *Pst*I linker sequence in the cDNA. Additional T7-based subclones were constructed by inserting HRV14 cDNA corresponding to the 3′ end of 3D^{pol}-coding sequence from *Hpa*I (nt 6338), *Xmn*I, (nt 7073), *Rsa*I (nt 7136), and *Ava*II (nt 7156) into the *Hpa*I site at nt 7169 into the pT7RV7168A+ plasmid linearized at the oligonucleotide-reconstructed *Hpa*I site to generate transcription vectors pT7RV6338A+, pT7RV7076A+, pT7RV7136A+, and pT7RV7152A+, respectively. The number in the plasmid nomenclature refers to the number of the first nucleotide of HRV14 sequence at the 5′ end of the transcript, disregarding a few additional nucleotides of vector sequence in some of the in vitro generated RNAs.

To generate RNAs which lacked the poly(A)$_n$ tract, the 3′ NCR cDNA was reconstructed with synthetic oligonucleotides RV3′NCR(+) (5′-AACAATAT AGACACTTAATTTGAGTAGAAGTAGGAGTTT**ATCGAT**CTGCA-3′) and RV3′NCR(−) (5′-G**ATCGAT**AAACTCCTACTTCTACTCAAATTAAGTGT CTATATTGTT-3′). These oligonucleotides included a *Hpa*I half-site, the complete HRV14 3′ NCR cDNA sequence, a *Cla*I site (indicated in boldface type), and a *Pst*I half-site to be inserted into the large fragment of the *Hpa*I/*Pst*I-digested poly(A)$_n^+$ transcription vectors to produce analogous poly(A)$^-$ constructs. The resulting plasmids were linearized with *Cla*I and used as T7 transcription templates to yield RNAs which contain only two extraneous nucleotides (-CG-3′) after the 3′ NCR sequence which are derived from the restriction site.

A portion of the cDNA corresponding to the HRV14 VP3 capsid protein-coding region from *Sca*I (HRV14 nt 1926) to *Hin*dIII (nt 2273) was also inserted into the pT7RV7168A− transcription vector upstream of the existing 3′ NCR cDNA sequence to allow the generation of RNAs VP3-3′NCR(A)$^-$, which contains sequences corresponding to part of the VP3-coding region juxtaposed to the HRV14 3′ NCR. The same cDNA sequence representing the VP3-coding region was also engineered into a transcription vector such that a VP3 transcript could be generated without the HRV14 3′ NCR sequence.

To construct a PV (type 1 Mahoney) transcription vector containing cDNA sequences corresponding to the 3′ NCR, a region of plasmid pMV7-2.9 (43) from *Pvu*II (PV1 nt 7053) to *Aat*II (pBR322 nt 4284) (containing cDNA sequences corresponding to the 3′ end sequences of PV1) was incubated in the presence of T4 DNA ligase with the fragment of the transcription vector pT7RV7168A+ containing the engineered T7 promoter from *Aat*II (pGEM1 nt 2085) to the reconstructed HRV14 *Hpa*I site at HRV14 nt 7169. The resulting plasmid, pT7MV7053A+, was linearized at a unique *Eco*RI site downstream of the PV1 poly(A)$_n$ tract to generate runoff transcripts containing sequences corresponding to 317 nt of 5′-proximal PV1 3D^{pol}-coding sequence, the PV1 3′ NCR, and a poly(A)$_n$ tract of ~60 to 80 nt.

Mutagenesis of viral cDNA constructs. A deletion mutation in the cDNA corresponding to the HRV 3′ NCR was generated by the method described in reference 29. Briefly, two oligonucleotides were designed such that the 5′ ends flanked a 7-nt target sequence (5′-ATATAGA-3′) to be deleted in the plasmid DNA corresponding to the HRV14 3′ NCR (see Results for the rationale). Oligonucleotides RV10Δ(−) (5′-TGTTAACCTAAAAGAGGTCC-3′) and RV11Δ(+) (5′-**C**ACAATTAAACTCATCTTCA-3′) were then annealed to the denatured plasmid pT7RV7076A+. A linear double-stranded DNA which lacked the nucleotides targeted for deletion fragment was then amplified by PCR. The linear fragment was incubated with T4 DNA ligase and then transformed into *E. coli* C600 cells. The resulting pT7RV7076A+(Δ8) deletion construct had 8 nt deleted (5′-ATATAGA**C**-3′), presumably as a result of slight oligonucleotide breathing between the 5′ end of RV11Δ(+) and the denatured plasmid (the boldface **C** above was also deleted). This 8-nt deletion was also inserted into the full-length viral cDNA clone pT7RV(FL) by insertion of a *Hpa*I fragment (HRV14 nt 6338 to 7169) into the pT7RV7076A+(Δ8) plasmid at the reconstructed *Hpa*I site, to generate pT7RV6338A+(Δ8), followed by cloning of an HRV14 cDNA-containing fragment of pT7RV6338A+(Δ8), from an *Sph*I site at HRV14 nt 6636 to the pGEM1 vector *Pvu*I site (nt 1537), into the corresponding sites in the full-length cDNA clone. The resulting plasmid, pT7RV(Δ8), was used to produce full-length RNAs bearing the Δ8 mutation in vitro for transfection studies.

In vitro RNA transcription and UV cross-linking assays. Transcription of high-specific-activity [α-^{32}P]GTP- or [α-^{32}P]UTP-radiolabeled RNAs and UV cross-linking were performed essentially as described in reference 40 with some minor modifications. Typically, only 0.25 to 1.0 pmol of radiolabeled probe was used per cross-linking reaction with 16 to 40 μg of S10 cytoplasmic cellular extract. A 20- to 40-μg (final concentration, 2 to 4 μg/μl) portion of poly(I-C) (Sigma) was added to each binding reaction simultaneously with the radiolabeled probe unless other unlabeled competitor RNAs were present. In this case, all competitor RNAs, including poly(I-C), were preincubated with the extract prior to the addition of probe as described in reference 40. For the generation of attenuator RNAs (the attenuator structure of the *E. coli ilvG-MEDA* operon), plasmid pTZl1 was obtained from Bhavin Parekh and G. Wesley Hatfield and was linearized with *Dra*I prior to use as a T7 transcription template (36).

Virus transfection, propagation, and plaque assays. In vitro synthesis of RNAs for virus transfection, DEAE-dextran-mediated transfection, plaque purification, preparation of virus stocks, and plaque assays have been previously described (12). Modifications of these procedure to accommodate HRV14 growth requirements include the following. (i) Rhinovirus was grown at 33°C in modified Eagle's minimal essential medium (Flow Laboratories) with 10% newborn bovine serum (Gibco), 1% minimal essential medium nonessential amino acids (Gibco), supplemented with 10 mM $MgCl_2$ and 20 mM *N*-2-hydroxyethylpiperazine-*N*′-2-ethanesulfonic acid (HEPES; pH 7.4) (19, 21). (ii) A HeLa cell variant (R19) was used for all monolayer cell culture work. This cell line supports the rapid growth of rhinovirus (1). (iii) When required for >48-h cell culture incubations, monolayers were fed or overlaid with fresh medium every 2 days. (iv) Plaque assays were fixed with 25% trichloroacetic acid usually at least 5 days following infection prior to staining with crystal violet.

Slot blot analysis. Total cytoplasmic RNA was prepared by the Nonidet P-40–sodium dodecyl sulfate (SDS) lysis method modified from that of Campos and Villarreal (11). RNA was extracted from HeLa R19 cells at various times following an infection by wild-type or Δ8 HRV14 at a multiplicity of infection of 0.5. Then 5 μg of RNA was slot blotted in glyoxal-dimethyl sulfoxide onto GeneScreen Plus (NEN) hybridization membrane with the Minifold II Slot-Blot System (Schleicher & Schuell) and probed with the [γ-^{32}P]ATP 5′-end-labeled HRV14-specific synthetic oligonucleotide RV4(−) (complementary to nt 283 to 302 in the 5′ NCR). Hybridization and washing conditions were as described in reference 12. The blot was then exposed to X-ray film. The resulting autoradiogram was scanned with an LKB Ultroscan II laser densitometer.

Sequencing of virus RNAs. HeLa R19 monolayers were infected at a multiplicity of infection of <1 with wild-type (wt) or Δ8 HRV14 recovered from RNA transfections. Following the onset of cytoplasmic effects, cellular RNA was prepared by the Nonidet P-40–SDS lysis method modified from that of Campos and Villarreal (11). An asymmetric reverse transcriptase-PCR technique was then used to specifically amplify cDNA sequences corresponding to the 3′ end of viral

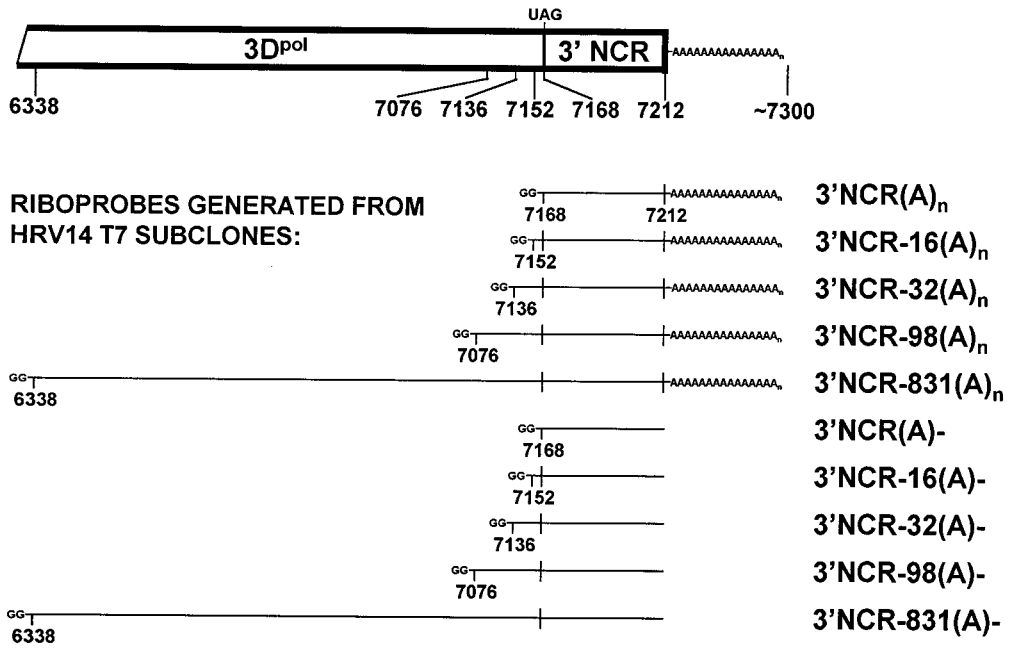

FIG. 1. Schematic diagram of the virus-specific RNAs used in UV cross-linking studies. All RNAs were generated in vitro as runoff transcripts from the T7-based cDNA transcription vectors described in Materials and Methods. The nomenclature of the transcribed RNAs denotes the number of nucleotides of RNA sequence which are 5′ proximal to the HRV14 RNA 3′ NCR (representing $3D^{pol}$-coding sequence) and the presence or absence of a 3′-terminal poly(A)$_n$ tract [e.g., 3′NCR-98(A)$_n$ contains an HRV14 RNA 3′ NCR, 98 nt of 5′-proximal sequence, and a poly(A)$_n$ tract]. Linearized plasmids pT7RV7168A+, pT7RV7152A+, pT7RV7136A+, pT7RV7076A+, pT7RV6338A+ pT7RV7168A−, pT7RV7152A−, pT7RV7136A−, pT7RV7076A−, and pT7RV6338A− were used as templates to generate RNAs 3′NCR(A)$_n$, 3′NCR-16(A)$_n$, 3′NCR-32(A)$_n$, 3′NCR-98(A)$_n$, 3′NCR-831(A)$_n$, 3′NCR(A)$^-$, 3′NCR-16(A)$^-$, 3′NCR-32(A)$^-$, 3′NCR-98(A)$^-$, and 3′NCR-831(A)$^-$, respectively. Additional RNAs are described in the text.

RNAs from the total cytoplasmic RNA. Oligonucleotide primers RV7035(+) (5′-GCATGTTAGCATGGCACTCAGG-3′), corresponding to nt 7035 to 7056 of HRV14, and RVoligoT+9(−) (5′-TTTTTTTTATAAACTCC-3′), complementary to nt 7204 to 7212 [and an additional 7 nt of the 3′-terminal poly(A)$_n$ tract], were first used at equal concentrations in a symmetric reverse transcriptase-PCR (46) to amplify a cDNA fragment corresponding to the target region of viral RNA [~200 ng of RNA, 10 U of avian myeloblastosis virus reverse transcriptase (Life Sciences), 13 U of RNasin (Promega), 2.5 U of *Taq* DNA polymerase (Boehringer Mannheim), 0.2 mM deoxynucleoside triphosphates (Pharmacia), 0.36 μM RV7035(+), 0.36 μM RVoligoT+9(−), 1× buffer (10 mM Tris-HCl, 1.5 mM $MgCl_2$, 50 mM KCl; pH 8.3) (Boehringer Mannheim) in a volume of 30 μl]. The same primers were subsequently used at a 10:1 ratio [0.36 μM RVoligoT+9(−), 36 pM RV7035(+)] in a second, asymmetric, PCR (with <10% of the first PCR mixture as a template) to asymmetrically amplify and enrich for the RVoligoT+9(−)-primed DNA strand. The predominant single-stranded DNA was then sequenced by using the modified T7 DNA polymerase (Sequenase; United States Biochemical) with oligonucleotide RV7035(+) as a primer.

RESULTS

Overview of the experimental scheme. To identify viral and/or cellular proteins which interact with the 3′ end of viral genomic RNAs to effect viral replication, an in vitro biochemical approach was used to study RNA-protein interactions. A nested series of T7-based transcription vectors was engineered to serve as templates for the generation of virus-specific RNAs in vitro. These RNAs represented the HRV14 3′ NCR plus various lengths of upstream (5′-proximal) $3D^{pol}$-coding sequence. RNAs could be generated such that they contained a 3′ poly(A)$_n$ tract (~60 to 90 nt) or terminated immediately after the 3′ NCR without a poly(A)$_n$ tract (Fig. 1). A UV cross-linking assay was then used with these RNAs and cytoplasmic cellular extracts from uninfected and virus-infected HeLa cells. With this assay, cellular proteins were detected in extracts from virus-infected cells which cross-linked to the HRV14-specific RNAs.

The specificity of the visualized proteins cross-linked to the 3′ NCR-containing RNAs was demonstrated by competition experiments with unlabeled HRV14-specific homologous competitor RNAs as well as several heterologous, irrelevant RNAs. RNAs were also engineered which placed the HRV14 3′ NCR in an altered context outside of the other HRV14 genomic 3′-end sequences to demonstrate that the 3′ NCR was the specific binding determinant required for efficient cross-linking of the cellular proteins. Finally, a mutated HRV14 3′ NCR was engineered which was predicted not to be recognized as a substrate for a viral replication initiation complex. RNAs containing this mutation were used in UV cross-linking assays and in transfection experiments to determine the effects of such a mutation on protein binding, virus infectivity, and viral RNA synthesis.

UV cross-linking of HRV poly(A)$^-$ RNAs to cellular polypeptides. Initial cross-linking studies were performed with virus-specific RNAs which lacked poly(A)$_n$ tracts. Our preliminary cross-linking experiments suggested that poly(A)$_n$-containing RNA probes interacted with a large number of cellular proteins and were not suitable for cross-linking analysis. However, in subsequent experiments, poly(A)-containing RNAs were used (see below). Figure 2 shows the results of a UV cross-linking assay in which RNAs 831-3′NCR(A)$^-$ (lanes 1 to 3), 98-3′NCR(A)$^-$ (lanes 4 to 6), 36-3′NCR(A)$^-$ (lanes 7 to 9), 16-3′NCR(A)$^-$ (lanes 10 to 12), and 3′NCR(A)$^-$ (lanes 13 to 15) were cross-linked in the absence of cellular extract (lanes −) or in the presence of extract from uninfected (lanes U) or HRV14-infected (lanes I) cells. The 3′NCR(A)$^-$ RNA represents the 3′ NCR with no additional flanking sequences. The

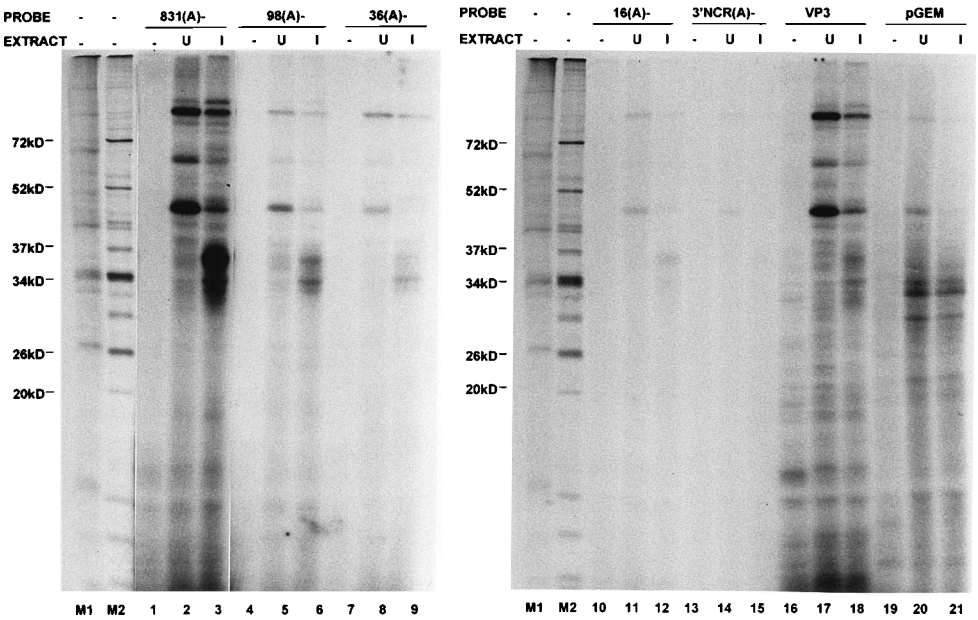

FIG. 2. UV cross-linking of HRV14 3′NCR(A)$^-$ probes containing decreasing lengths of proximal 3D sequences. In vitro transcribed RNAs (1 pmol) were incubated in the absence of HeLa cell extract (lanes −), in the presence of 40 μg of extract from uninfected cells (lanes U), or in the presence of 40 μg of extract from HRV14-infected cells (lanes I). HRV and PV markers are shown (lanes M1 and M2, respectively). Other lanes show ^{32}P-labeled probes: 3′NCR-831(A)$^-$ (lanes 1 to 3), 3′NCR-98(A)$^-$ (lanes 4 to 6), 3′NCR-36(A)$^-$ (lanes 7 to 9), 3′NCR-16(A)$^-$ (lanes 10 to 12), 3′NCR(A)$^-$ (lanes 13 to 15), VP3 (lanes 16 to 18), and pGEM (lanes 19 to 21), incubated as described in Materials and Methods. Samples were then boiled and resolved on a 12.5% polyacrylamide gel under denaturing conditions. The exposure time for lanes 1 to 3 was approximately one-third that used for the remaining lanes.

appearance of complexes in the range of 34 to 36 kDa correlates with the use of the longer 3′ NCR-containing RNAs and extract from infected cells (lanes 3 and 6). These complexes also appear, but at greatly reduced levels, when extracts from uninfected cells are used (lanes 2 and 5), suggesting that the proteins are of cellular origin and are sequestered or modified in infected cells, to make them available to interact with viral RNAs. Two irrelevant RNAs, VP3 (representing part of the coding region for the HRV14 capsid protein VP3) and pGEM (vector sequence from pGEM1 [Promega]), were used as nonspecific cross-linking controls (lanes 16 to 21). These RNAs would not be expected to specifically interact with proteins involved in rhinovirus replication. Indeed, cross-linking of the cellular factors to these RNAs was very inefficient although detectable in some experiments. Pretreatment of cellular extracts with proteinase K prior to use for UV cross-linking or treatment of the cross-linked RNA-protein products following UV irradiation with proteinase K completely eliminated the appearance of the visualized bands, demonstrating that the observed radiolabeled species was indeed an RNA-protein complex (data not shown). Although the cellular protein(s) sometimes appears as more than a single distinct band by SDS-polyacrylamide gel electrophoresis, especially when greater quantities of cellular extract are used, it will be considered a single protein complex for the purposes of this report. The appearance of more than one band may be due to differential efficiency of RNase digestion, leaving longer RNA fragments covalently attached to some proteins in a population, or to the lability of the protein in question (perhaps as a consequence of UV irradiation); either of these explanations could account for the appearance of up to four tightly spaced bands on some autoradiograms. An approximately 50-kDa protein is also observed as one of the more intense bands on the autoradiogram. This protein is nonspecifically cross-linked to almost any radiolabeled RNA and will not be discussed further.

Specificity of the cellular protein(s) for RNAs containing the HRV14 3′ NCR. To establish that the protein(s) visualized by UV cross-linking was specific for the 831-3′NCR(A)$^-$ RNA, competition experiments were conducted with increasing molar excesses of the homologous unlabeled RNA (Fig. 3, lanes 3 to 6) and heterologous VP3 RNA (lanes 7 to 10). While a 10-fold molar excess of homologous unlabeled RNA competes readily for binding of the 34- to 36-kDa protein(s) (lane 6), the nonspecific competitor competes much less efficiently (lane 10). More efficient competition with the homologous competitor RNA was also observed at lower levels of unlabeled RNA (compare lanes 3 to 5 with lanes 7 to 9). This experiment has been repeated four times with similar results. These data suggest a binding preference of the cellular proteins for the 3′ NCR-containing RNA.

Context and 3′ NCR specificity determinants for protein complex formation. To examine the possibility that 5′-proximal 3D^{pol} sequences and not the 3′ NCR sequences were responsible for binding of the cellular proteins to HRV14-specific RNAs, radiolabeled RNAs were used in which the 5′-flanking polymerase-coding sequence had been replaced with RNA corresponding to VP3-coding sequence. The VP3-3′NCR(A)$^-$ RNA contains the same VP3 sequence described above immediately upstream of the HRV14 3′ NCR. Figure 4A shows results of UV cross-linking and corresponding competition experiments with these RNAs. Lanes 1 to 6 show cross-linking of VP3, 831-3′NCR(A)$^-$, and VP3-3′NCR(A)$^-$ RNAs, respectively, in the presence of extract from uninfected (U) and infected (I) cells. Efficient cross-linking of the 34- to 36-kDa protein was seen only with the 3′ NCR-containing RNA, 831-3′NCR(A)$^-$ (lane 4). An additional protein species (indicated by the small arrow in Fig. 4A) was cross-linked to the VP3-3′NCR(A)$^-$ probe, as well as to the 831-3′NCR(A)$^-$ probe, primarily from extracts from infected cells (lanes 4 and 6). The VP3 RNA did not interact with the cellular factors itself (lane 2) but appeared to function weakly as a 5′-flanking sequence to

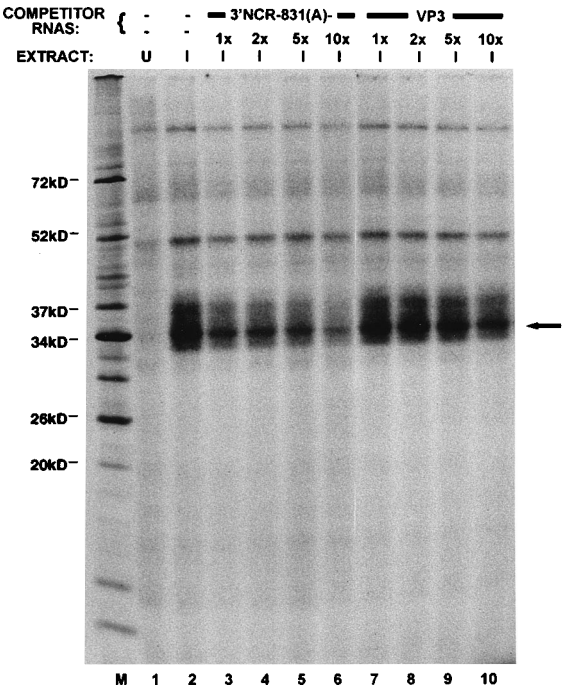

FIG. 3. UV cross-linking competition assay. Unlabeled 3′NCR-831(A)$^-$ and VP3 were used as competitor RNAs at molar ratios of 1, 2, 5, and 10 with respect to ^{32}P-labeled 3′NCR-831(A)$^-$ probe (1 pmol). The total amount of extract used in each reaction was ~16 μg. Incubation of the labeled probe with extract from uninfected cells is shown in lane 1, followed by incubation with extract from HRV14-infected cells (lane 2) with no specific competitor RNAs. The remaining lanes show incubations with increasing concentrations of homologous competitor, 3′NCR-831(A)$^-$ (lanes 3 to 6), or increasing concentrations of nonspecific competitor, VP3 (lanes 7 to 10), in extract from infected cells. The arrow indicates the RNA-protein complex with a binding preference for the 3′NCR-831(A)$^-$ RNA.

allow the 3′ NCR to interact with the cellular proteins. The corresponding competition experiment (lanes 7 to 12) further demonstrates the specificity of the cross-linked proteins for the HRV14 3′ NCR. In this part of the assay, radiolabeled probe 831-3′NCR(A)$^-$ was used with the competitors VP3 (lanes 7 and 8), 831-3′NCR(A)$^-$ (lanes 9 and 10), and VP3-3′NCR(A)$^-$ (lanes 11 and 12). Competition for the cellular factor(s) with unlabeled VP3 was inefficient, even at a 50-fold molar excess of VP3 (lane 8). Competition with the 3′ NCR-containing RNA, 831-3′NCR(A)$^-$, is markedly more efficient than with an RNA containing VP3 sequences (lanes 9 and 11). The VP3-3′NCR(A)$^-$ RNA competes less efficiently than the homologous 831-3′NCR(A)$^-$ RNA but better than the VP3 RNA. The results of these binding and competition experiments demonstrate that the 3′ NCR is the important binding determinant for molecular recognition by the cellular protein(s). A substantial 5′-flanking sequence is required for efficient UV cross-linking; however, there does not appear to be a strict sequence requirement for this upstream sequence. The nucleotide sequence upstream of the 3′ NCR may provide a tethering role for the molecular recognition by cellular factors.

Since viral genomic RNAs contain a genetically encoded poly(A)$_n$ tract, it was desirable to use polyadenylated radiolabeled RNAs in the cross-linking assays to investigate the role of 3′-terminal homopolymeric sequences on the observed RNA-protein interactions. By using [α-^{32}P]UTP instead of [α-^{32}P]GTP as the source of radiolabel, 3′-end labeling of RNase-resistant poly(A)$_n$ tracts via the incorporation of label into the terminal G residue from the *Pst*I restriction site (used to linearize plasmids for transcription) was avoided. Through this procedural modification, the use of polyadenylated RNAs in the cross-linking assay became possible.

To investigate the role of the 3′ virus-encoded polyadenosine tract in the observed RNA-protein interactions, [α-^{32}P]UTP-radiolabeled RNAs were used which included a ~60 to 80-nt poly(A)$_n$ tract. Both the 831-3′NCR(A)$_n$ and the 98-3′NCR(A)$_n$ RNAs cross-linked to the 34- to 36-kDa proteins efficiently (Fig. 4B, lanes 10 and 12). Although it is not required for binding of the cellular factors, the addition of the poly(A)$_n$ tract to the 98-3′NCR RNA sequence did appear to enhance its cross-linking efficiency to a level comparable to that of the 831-3′NCR(A)$_n$ RNA. Experiments to quantitatively assess the cross-linking contribution to the binding of the cellular factor have not been performed, since the 3′ NCR was necessary and sufficient for binding (see Discussion). Competition experiments with commercially available unlabeled poly(A)$_n$ RNA (Sigma) demonstrated that the poly(A)$_n$ tract was not the binding determinant for the RNA-protein interaction. The autoradiogram in Fig. 4B shows cross-linking in the presence of increasing amounts of competitor, up to approximately 100-fold molar excess in lanes 1 to 4. Specific competition was not observed for the HRV14-specific radiolabeled RNAs. Thus, while the presence of the poly(A)$_n$ tract in RNAs containing the HRV14 3′ NCR increased the cross-linking efficiency of these RNAs to the cellular factors, the 3′ NCR was the primary binding determinant for the interaction.

Generation of a deletion mutation in the HRV14 3′ NCR. To better define the molecular genetic requirements involved in the recognition of the 3′ NCR by the cellular protein, we engineered a deletion into the HRV14 3′ NCR. A highly conserved 7-nt sequence was identified in the 3′ NCRs of RNAs from four HRVs, HRV1B (28), HRV2 (44), HRV14 (10), and HRV89 (20). Figure 5A shows a computer-generated (27) and manually adjusted sequence alignment of the 3′ NCRs of these four rhinoviruses. The larger gray box indicates the highly conserved RNA sequence chosen for deletion in the 3′ NCR of HRV14. This deletion also drastically changes the computer-predicted (47) secondary structure of the HRV14 3′ NCR (data not shown). The deletion was generated as described in reference 29, with specific details described in Materials and Methods. Presumably as the result of "breathing" at the 3′ end of oligonucleotide HRV10Δ(−) and the plasmid sequences corresponding to the 3′ NCR of HRV14, an 8-nt deletion (referred to as Δ8) was obtained as the de facto mutation, which was subsequently used for the studies described below.

Characterization of the Δ8 mutation by UV cross-linking. To study the effects of the 3′ NCR deletion on binding of the cellular factor(s) in the UV cross-linking assay, [α-^{32}P]UTP-radiolabeled 98-3′NCR(A)$_n$ RNAs with either a wt or Δ8 3′ NCR were generated and subjected to UV cross-linking in the presence of S10 extracts from HeLa cells. Figure 5B shows the results of a UV cross-linking experiment with these RNAs (lanes 1 to 4), as well as two additional nonspecific control RNAs, 98(*Ava*II) (lanes 5 and 6) and *atten* (lanes 7 and 8). The 98(*Ava*II) RNA contains only the 5′-proximal sequence with no 3′ NCR. The *atten* RNA represents the 186-nt attenuator structure of the *E. coli ilvGMEDA* operon as a control RNA with elaborate secondary structure. The Δ8 3′ NCR formed a UV-inducible complex with the cellular protein(s) with approximately 35% efficiency (lanes 3 and 4) compared with the wt 3′ NCR (lanes 1 and 2). This differential cross-linking between the wt and Δ8 3′ NCRs was observed reproducibly in three independent experiments. Only slight background cross-

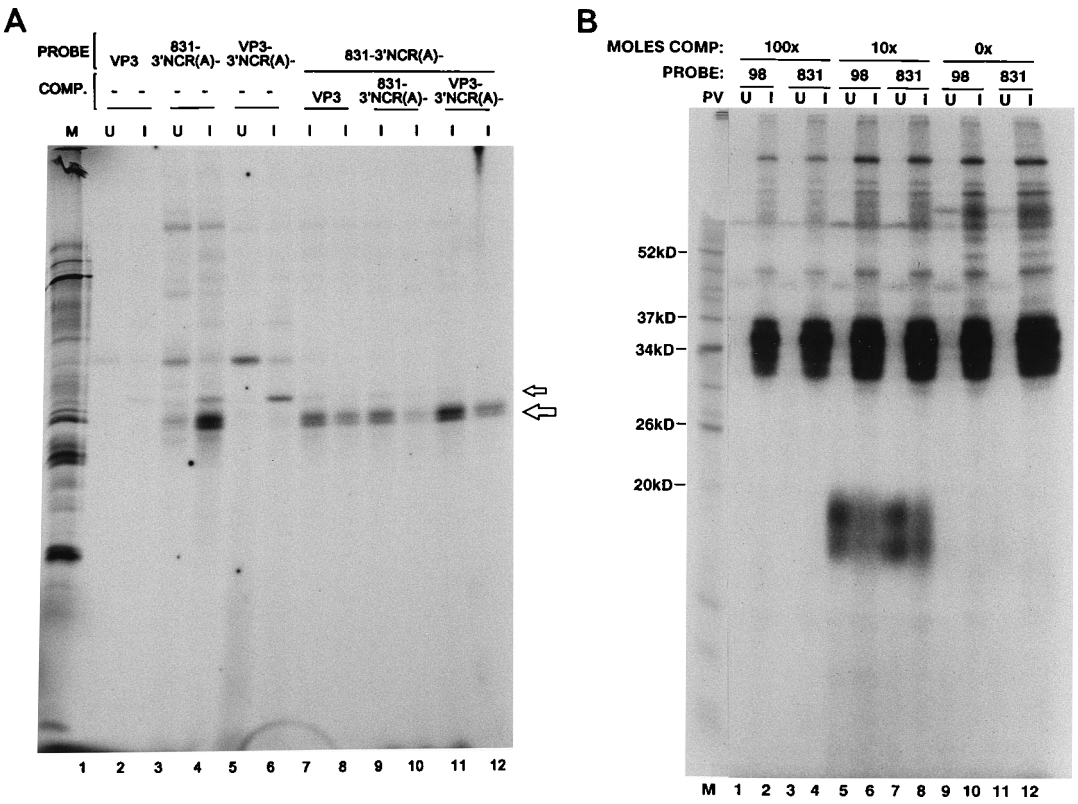

FIG. 4. Specificity of the cellular protein(s) for RNAs containing the HRV14 3′ NCR. (A) Binding and competition with unlabeled VP3, 3′NCR-831(A)$^-$, or 3′NCR-VP3(A)$^-$ RNAs at 5- and 50-fold molar ratios with respect to labeled 3′NCR-831(A)$^-$ probe (0.5 pmol). Cross-linking with labeled VP3, 3′NCR-831(A)$^-$, and 3′NCR-VP3(A)$^-$ with 16 μg of extract from uninfected (lanes U) or infected (lanes I) cells is shown (lanes 1 to 6), followed by cross-linking competitions with unlabeled RNAs, in the same order of addition, in extracts from infected cells: VP3 (lanes 7 and 8), 3′NCR-831(A)$^-$ (lanes 9 and 10), and 3′NCR-VP3(A)$^-$ (lanes 11 and 12), at 5- and 50-fold molar excesses, respectively. The large arrow indicates the 34- to 36-kDa proteins discussed elsewhere in the text. The small arrow indicates an additional radiolabeled species, which is observed in UV cross-linking assays with 3′ NCR-containing RNAs. (B) Cross-linking competition assay with 3′NCR-831(A)$_n$ and 3′NCR-98(A)$_n$ radiolabeled RNAs without competitor RNA (lanes 9 to 12) and with a 10- or 100-fold molar excess of unlabeled poly(A)$_n$ (lanes 1 to 8) in the presence of extract from uninfected (lanes U) or infected (lanes I) cells.

linking (<10%) was observed with the RNAs which did not contain a rhinovirus 3′ NCR (lanes 5 to 8). A competition cross-linking experiment was also performed (Fig. 5C) with [α-^{32}P]UTP-radiolabeled wt 98-3′NCR(A)$_n$ RNA as the probe and unlabeled wt 98-3′NCR(A)$_n$ (lanes 2 and 3), Δ8 98-3′NCR (A)$_n$ (lanes 4 and 5), 98(*Hpa*I) (lanes 6 and 7), or VP3 (lanes 8 and 9) RNAs as competitors. The 98(*Hpa*I) RNA contains an additional 11 nt of HRV14 3D^{pol}-coding sequence at the 3′ end of the transcript compared with the 98(*Ava*II) RNA as a result of linearization of the pT7RV7076A+ transcription vector with the restriction enzyme *Hpa*I (HRV14 nt 7169) instead of *Ava*II (nt 7156). Both RNAs represent the HRV14 3D^{pol}-coding sequences proximal to (but not including) the 3′ NCR. Only the wt 3′ NCR competed efficiently for binding with the radiolabeled probe (lanes 2 and 3), indicating that the intact HRV14 3′ NCR is the RNA-binding determinant for the cellular protein. On the basis of densitometric scanning of five similar competition experiments, the Δ8 3′ NCR competed only ~25% as efficiently as did the wt 3′ NCR for binding of the cellular factor(s) to the wt probe.

In vivo characterization of the Δ8 mutation. The Δ8 mutation was introduced into full-length HRV14 cDNAs as described in Materials and Methods. Full-length wt and Δ8 RNAs were generated in vitro and transfected into HeLa R19 tissue culture cells which were then overlaid with liquid or semisolid medium and incubated at 33°C. Virus was recovered from both wt and Δ8 RNA transfections. Four individual plaque-purified Δ8 viruses were used to prepare virus stocks, in parallel with plaques derived from wt virus. Sequencing of these four Δ8 transfection-derived viruses demonstrated that they retained the originally engineered Δ8 mutation. While the titers of wt HRV14 P1 and P2 stocks were consistently 1×10^8 to 3×10^8 PFU/ml, Δ8 stocks ranged from ~5×10^6 to 1×10^7 PFU/ml (~1 to 1.5 log units lower). Δ8 virus exhibited a small-plaque phenotype after 5 days under semisolid overlay, as shown in Fig. 6.

To demonstrate that the nature of the Δ8 virus defective growth phenotype was a replication defect, RNA slot blot analysis was performed on total RNA harvested from wt and Δ8 HRV14-infected cells to monitor the time of onset and maximum levels of viral RNA for up to 38 h postinfection (p.i.). As shown in Fig. 7A, the Δ8 virus demonstrated both delayed onset and decreased levels of accumulated cytoplasmic RNA compared with wt HRV14. wt viral RNA is readily detectable at 12 h p.i., whereas Δ8 virus is barely detectable at 12 h p.i. but visible at 18 h p.i. The maximum RNA level detected in Δ8-infected cells at 38 h p.i. is ~75% of the wt level at 30 h p.i., as determined by densitometric scanning of the autoradiogram (Fig. 7B). As a consequence of the location of the engineered Δ8 lesion and the demonstration of delayed onset and accumulation of viral RNA within infected cells, we suggest that the mutant phenotype is due to alterations in the molecular recognition of the 3′ NCR by cellular and, perhaps, viral proteins involved in RNA replication.

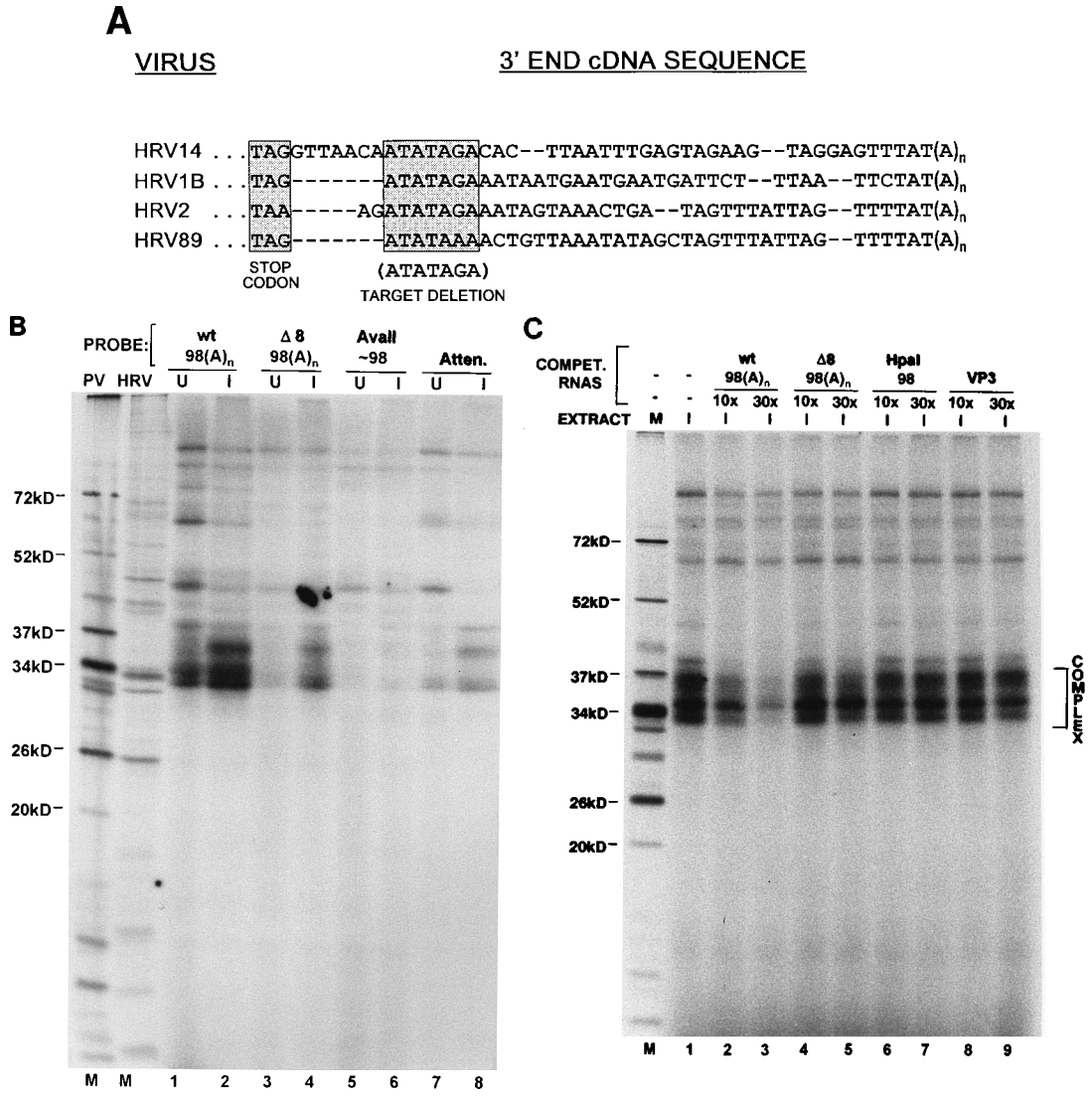

FIG. 5. UV cross-linking with an HRV14 RNA 3′ NCR deletion mutation. (A) The RNA 3′ NCRs of HRV1B, HRV2, HRV14, and HRV89 are shown in a manually adjusted Clustal (27) alignment. The left-most shaded box indicates the STOP codon at the end of the RNA $3D^{pol}$-coding sequence. The second shaded box indicates a highly conserved sequence (5′-ATATAGA-3′), which was selected as the target for mutagenesis in the HRV14 RNA 3′ NCR. (B) UV cross-linking with the Δ8 3′ NCR mutated RNA. Lanes: 1 and 2, radiolabeled wt 3′NCR-98$(A)_n$ RNA incubated with extract from uninfected (U) or infected (I) cells; 3 and 4, Δ8 3′NCR-98$(A)_n$ RNA; 5 and 6, 98(*Ava*II) RNA; 7 and 8, a secondary-structure control RNA (attenuator structure of the *ilvGMEDA* operon in *E. coli*. (C) Competition cross-linking experiment with [α-^{32}P]UTP-radiolabeled wt 98-3′NCR$(A)_n$ RNA as the probe and unlabeled wt 98-3′NCR$(A)_n$ (lanes 2 and 3), Δ8 98-3′NCR$(A)_n$ (lanes 4 and 5), 98(*Hpa*I) (lanes 6 and 7), or VP3 (lanes 8 and 9) RNA as competitors.

Cellular protein-viral RNA complex formation following picornavirus infections of HeLa cells. We also investigated the binding of cellular proteins to the 3′ end of PV1 genomic RNAs to determine if RNA-protein complexes were observed with PV1-specific RNAs which were analogous to those seen with HRV14-specific RNAs. Figure 8A shows a cross-linking experiment involving the previously described HRV14 probe 98-3′NCR$(A)_n$ (lanes 1 to 3) and the PV1 probe 317-3′NCR $(A)_n$ (lanes 4 to 6), which contains the 72-nt PV1 3′ NCR, 317 nt of PV1 5′-flanking polymerase $3D^{pol}$ sequence, and a ~50- to 80-nt 3′ poly$(A)_n$ tract. These radiolabeled RNAs were incubated with extracts from uninfected (U), HRV14-infected (HRV), or PV1-infected (PV) cells. Although the overall binding patterns are different, complexes of proteins (34 to 36 kDa) with similar electrophoretic properties are visible when either virus-specific RNA was used with extracts from either HRV14- or PV1-infected HeLa cells. UV cross-linking competition experiments (results not shown) demonstrated that the two different 3′ NCRs could also efficiently compete with one another for binding to the cellular factor compared with a nonspecific competitor RNA corresponding to HRV14 VP3. This finding suggests that the appearance of the cellular protein may be a more general result of picornavirus infection and not unique to HRV14.

We also monitored the appearance of the cellular protein during the course of a viral infection. In the time course experiment in Fig. 8B, S10 cytoplasmic extracts were prepared from PV1-infected HeLa cells every 30 min p.i. for up to 5 h. These extracts were then used for cross-linking with a PV1 3′ NCR-specific probe. The appearance of the 34- to 36-kDa complex correlates with the time of peak PV RNA replication at ~4 to 4.5 h p.i. (15, 16) (Fig. 8B, lanes 10 and 11). This

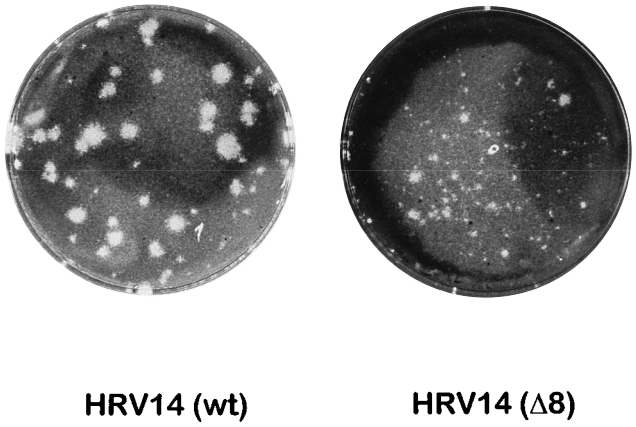

FIG. 6. Plaque morphology of wt and Δ8 HRV14. Infected HeLa (R19) monolayers were overlaid with semisolid agar overlay in Eagle's minimal essential medium. Monolayers were fed 2 and 4 days p.i. with an additional 4 ml of medium, fixed with 2 to 3 ml of 25% trichloroacetic acid, and developed with crystal violet after 5 days.

finding is highly suggestive of a role for the cellular factor in viral RNA replication.

DISCUSSION

The experiments reported in this article were aimed at identifying viral and/or cellular factors which interact with the 3′ NCR of HRV14. We have used a UV cross-linking assay with radiolabeled HRV14 3′-end-specific RNAs and extracts from human cells. A cellular factor(s) has been identified which interacts with the 3′ NCR of both HRV14 and PV1 genomic RNAs. The presence of this protein was demonstrable in extracts from cells infected with either virus. We suggest that the 34- to 36-kDa proteins are of cellular origin for at least three compelling reasons: (i) the proteins appear in low levels in extracts from uninfected cells; (ii) proteins with indistinguishable electrophoretic properties appear in extracts from HRV14-infected and PV1-infected cells (despite the fact that all HRV14 proteins have different molecular weights from PV1 proteins); and (iii) immunoprecipitations with antibody against PV1 proteins 2C, 3AB, $3C^{pro}$, $3D^{pol}$, 3CD, and the capsid proteins failed to immunoprecipitate any proteins cross-linked from extracts prepared from PV1-infected cells (data not shown). Our data imply that the cellular factor(s) observed in our cross-linking experiments is important for molecular recognition of the picornavirus genomic RNA by the viral replication complex in order to direct the specific replication of viral genomic RNAs within an infected cell.

The identification of a mechanism of RNA-protein recognition which confers specificity to the process of viral replication has become a fundamental issue in the understanding of picornavirus replication. Despite the recent technological advances which have allowed de novo synthesis of poliovirus in an in vitro system (5, 32), a picornavirus replication system with strictly defined components capable of specific recognition and amplification of viral RNAs has not been reconstituted. The virus-encoded RNA-dependent RNA polymerase ($3D^{pol}$) has been shown in vitro to be necessary and sufficient for elongation of an oligo(U)-primed polyadenylated RNA template, with some specificity for poliovirus RNAs (22); however, the viral polymerase can nonspecifically copy other polyadenylated RNAs which are not of viral origin when provided with an oligo(U) primer (17, 39) or a host factor (3, 18, 26). This latter

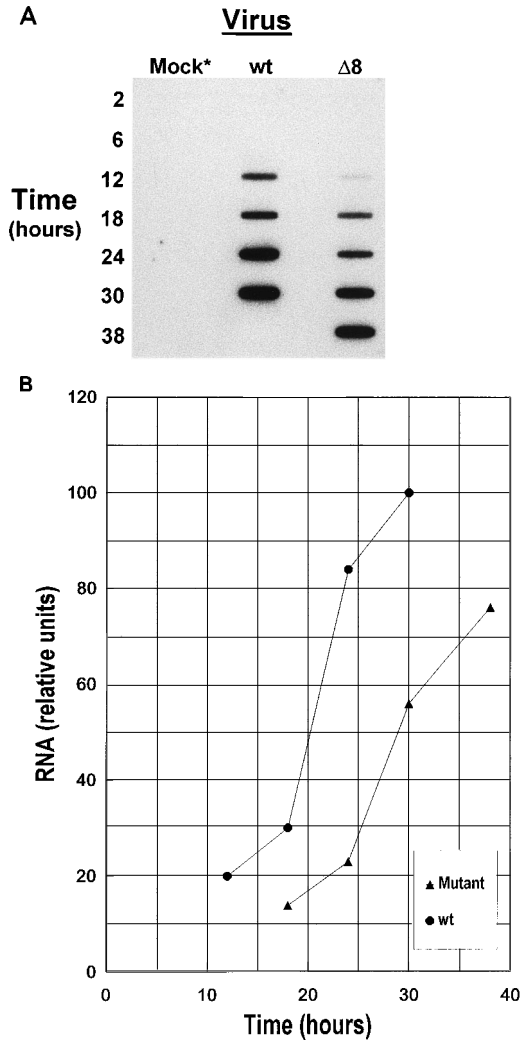

FIG. 7. (A) Slot blot analysis of wt and Δ8 HRV14 RNA replication. Total cytoplasmic RNA was harvested from HeLa (R19) monolayers 2, 6, 12, 18, 24, 30, and 38 h following infection with wt or Δ8 HRV14 at a multiplicity of infection of 0.5 or following mock infection. Then 5 μg of RNA was blotted onto a membrane, which was probed with a radiolabeled HRV14 plus-strand RNA-specific oligonucleotide, RV4(−). *, RNA harvests of mock-infected cell monolayers were made only at 12 and 24 h. (B) Results of densitometric scanning of the autoradiogram in panel A.

observation has led to the conclusion that there must be internal viral RNA-binding determinants, most likely in the 3′ NCR, which are responsible for conveying specificity to the assembly of the replication initiation complex (13). A site-directed mutation in the PV RNA 3′ NCR was reported that resulted in a temperature-sensitive defective RNA replication phenotype (42). More recently, 3′ NCR mutations which resulted in a defective replication phenotype in PV were correlated with disruptions of an elaborate secondary structure which has been computer predicted (37) and biochemically confirmed (30), indicating the presence of a pseudoknot structure within the 3′ NCR of PV genomic RNAs.

The observations reported here suggest the involvement of a cellular protein(s) in the specific recognition of the 3′ NCR of picornavirus RNAs in an infected cell. Such a viral RNA-cellular protein interaction may be exploited during the course of a viral infection to direct the specific assembly of a viral

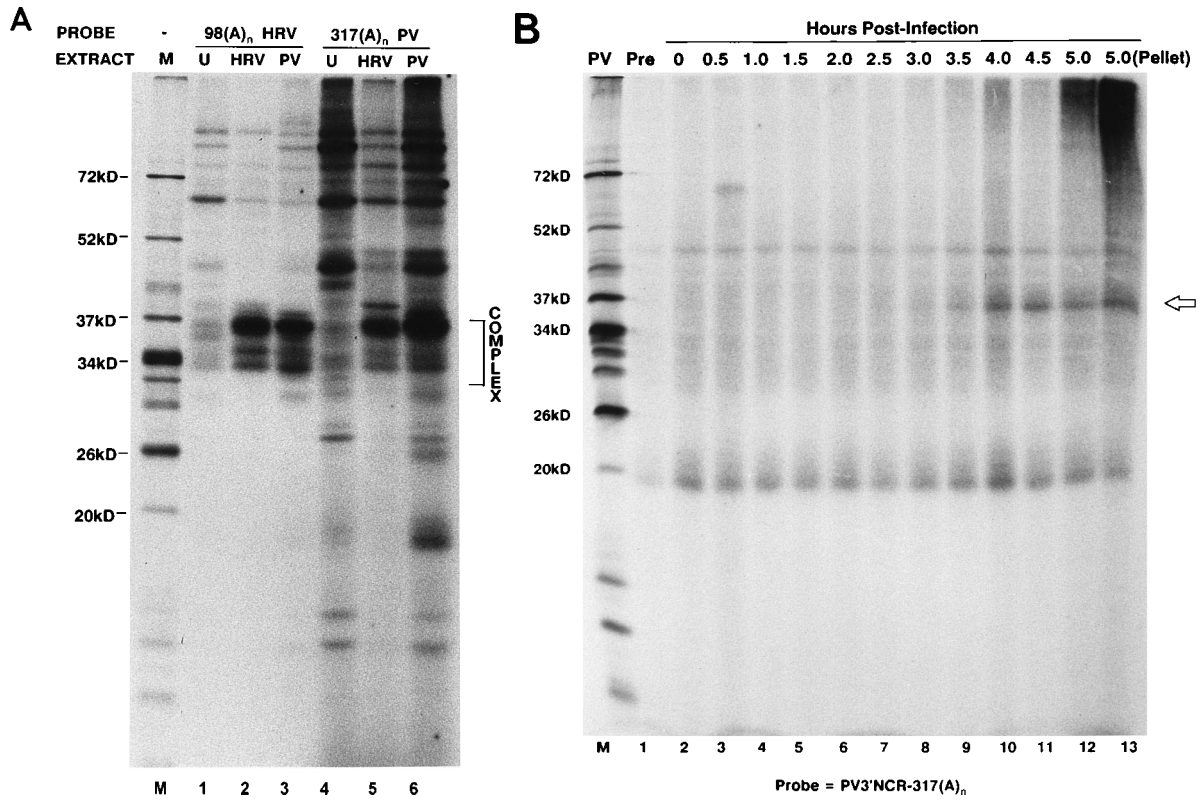

FIG. 8. UV cross-linking of HRV- and PV-specific RNAs. (A) HRV14-specific RNA 98-3′NCR(A)$_n$ (lanes 1 to 3) and PV1-specific RNA 317-3′NCR(A)$_n$ (lanes 4 to 6) incubated in the presence of extract from uninfected (lanes U), HRV14-infected (lanes HRV), or PV1-infected (lanes PV) cells. The electrophoretically indistinguishable RNA-protein complex(es) observed with HRV14 and PV1 RNA 3′ NCR-specific probes and extracts from virus-infected cells is indicated on the right margin of the figure. (B) PV time course cross-linking experiment. Cytoplasmic extracts were prepared every 30 min for up to 5 h following PV1 infection of HeLa cells in suspension culture at a multiplicity of infection of 20. The arrow to the right indicates the RNA-protein complex which appears during the course of infection.

RNA replication complex around a target viral RNA template. Such virus-cell interactions have been implicated in the replication of positive-strand RNA plant viruses, such as brome mosaic virus (38) and cucumber mosaic virus (25). Utilization of cellular proteins for the synthesis of plus-strand RNAs from intermediate minus-strand RNA templates has also been proposed for PV (2, 41) and Sindbis virus (35). While no direct functional assay has been described to demonstrate that the observed cellular factor is required for HRV or PV RNA replication, the involvement of this cellular protein is suggested by three lines of evidence. (i) The protein appeared in cytoplasmic extracts as the result of infection and at the peak RNA replication time (for PV) in a time course, UV cross-linking assay (Fig. 8B). (ii) The protein appeared as a result of either HRV14 or PV1 infection and had a marked binding preference for the 3′ NCR of the RNAs of these viruses. (iii) A deletion mutation in the 3′ NCR of HRV14 genomic RNA resulted in a virus with a defective RNA replication phenotype in vivo. This phenotype correlated with reduced binding efficiency of the cellular protein(s) to the mutated HRV14 RNA in an in vitro UV cross-linking assay. As our cross-linking assay was consistently incapable of detecting the interaction of the viral polymerase (3D^{pol}) or any viral protein with the 3′ NCR, it may be speculated that this cellular RNA-binding protein is recruited by picornaviruses as a prerequisite for the assembly of the replication initiation complex around the 3′ end of viral genomic RNAs or, alternatively, for the recognition of the target replication template by a viral replication complex which is already assembled. This explanation is consistent with the requirement for soluble host factors in the recent descriptions of de novo virus synthesis in vitro (5, 32).

Several explanations may be suggested to account for the appearance of the above-described cellular protein(s) in cytoplasmic extracts from virus-infected cells. (i) A cellular protein was modified as a result of viral infection (perhaps by a viral proteolytic activity) such that it could be utilized by the virus to effect replication. Recently, a 36-kDa cellular protein was reported to participate in the formation of a nucleoprotein complex that included in vitro generated RNAs corresponding to the 5′ end of PV positive-strand RNAs and partially purified, recombinant 3CD proteinase (2). There is evidence that this host cell protein is a cleavage product of the cellular translation factor, EF-1α (24). (ii) As the result of the gross architectural changes which occur within an infected host cell (33; for a review, see reference 39), the protein could be redistributed within the cell to become available to participate in viral replication. If the protein is normally associated with membranous vesicles, the budding and proliferation of smooth membranes within the cytoplasm of the infected cell may alter the compartmentalization of specific cellular proteins. The viral membrane-associated proteins, 2B, 2C, and 3A, may play a role in making cellular protein(s) available in membranous viral replication centers through as yet poorly defined activities (6, 23, 45). (iii) The synthesis of the observed cellular protein may be induced by the process of viral infection. This explanation would imply that translation of the protein occurred in a cap-independent manner. We currently favor the modification/se-

questration hypotheses for explaining the appearance of the cellular protein in extracts from virus-infected cells.

A recent report by Cui et al. has shown the encephalomyocarditis virus (EMCV) poly(A)$_n$ tract is required for the recognition of viral genomic 3′-end sequences by purified EMCV 3D^{pol} (14). This observation suggests that not only does the viral polymerase require the genetically encoded poly(A)$_n$ tract in the RNA template, but also that EMCV 3D^{pol} can inherently recognize internal genomic EMCV RNA sequences. As has been previously demonstrated in vitro, poliovirus 3D^{pol} can elongate primed templates of nonviral polyadenylated RNAs (17, 39). Therefore, there must be an additional mechanism by which substrate specificity is imparted to the HRV14 and PV1 viral replication initiation complex involving host factors and/or other viral proteins. Our report of a cellular protein with a binding preference for the HRV14 RNA 3′ NCR is consistent with this hypothesis.

ACKNOWLEDGMENTS

We thank Holger Roehl and Jon Towner for critical reading of the manuscript. We also thank Eckard Wimmer for communicating data from his laboratory prior to publication.

S.T. is a predoctoral trainee of a Public Health Service training grant (GM07134). This work was supported by Public Health Service grant AI22693 from the National Institutes of Health.

REFERENCES

1. **Abraham, G., and R. J. Colonno.** 1984. Many rhinovirus serotypes share the same cellular receptor. J. Virol. **51:**340–345.
2. **Andino, R., G. E. Rieckhof, P. L. Achacoso, and D. Baltimore.** 1993. Poliovirus RNA synthesis utilizes an RNA complex formed around the 5′-end of viral RNA. EMBO J. **12:**3587–3598.
3. **Andrews, N. C., and D. Baltimore.** 1986. Purification of a terminal uridylyl transferase that acts as a host factor in the *in vitro* poliovirus replicase reaction. Proc. Natl. Acad. Sci. USA **83:**221–225.
4. **Baltimore, D., Y. Becker, and J. E. Darnell.** 1964. Virus-specific double stranded RNA in poliovirus-infected cells. Science **14:**1034–1036.
5. **Barton, D. J., and J. B. Flanegan.** 1993. Coupled translation and replication of poliovirus RNA in vitro: synthesis of functional 3D polymerase and infectious virus. J. Virol. **67:**822–831.
6. **Bienz, K., D. Egger, M. Troxler, and L. Pasamontes.** 1990. Structural organization of poliovirus RNA replication is mediated by viral proteins of the P2 genomic region. J. Virol. **64:**1156–1163.
7. **Bishop, J. M., G. Koch, B. Evans, and M. Merriman.** 1969. Poliovirus replicative intermediate: structural basis of infectivity. J. Mol. Biol. **46:**235–249.
8. **Caliguiri, L. A., and I. Tamm.** 1970. The role of cytoplasmic membranes in poliovirus biosynthesis. Virology **42:**100–110.
9. **Caliguiri, L. A., and I. Tamm.** 1970. Characterization of poliovirus-specific structures associated with cytoplasmic membranes. Virology **42:**112–122.
10. **Callahan, P. L., S. Mizutani, and R. J. Colonno.** 1985. Molecular cloning and complete sequence determination of the RNA genome of human rhinovirus type 14. Proc. Natl. Acad. Sci. USA **82:**732–736.
11. **Campos, R., and L. P. Villarreal.** 1982. An SV40 deletion mutant accumulates late transcripts in paranuclear extract. Virology **119:**1–11.
12. **Charini, W. A., C. C. Burns, E. Ehrenfeld, and B. L. Semler.** 1991. *trans* rescue of a mutant poliovirus RNA polymerase function. J. Virol. **65:**2655–2665.
13. **Collis, P. S., B. J. O'Donnell, D. J. Barton, J. A. Rogers, and J. B. Flanegan.** 1992. Replication of poliovirus RNA and subgenomic RNA transcripts in transfected cells. J. Virol. **66:**6480–6488.
14. **Cui, T., S. Sankar, and A. G. Porter.** 1993. Binding of encephalomyocarditis virus RNA polymerase to the 3′-non-coding region of the viral RNA is specific and requires the 3′-poly(A) tail. J. Biol. Chem. **268:**26093–26098.
15. **Darnell, J. E., M. Girard, D. Baltimore, D. F. Summers, and J. V. Maizel.** 1967. The synthesis and translation of poliovirus RNA, p. 375–401. *In* J. S. Colter and W. Paranchych (ed.), The molecular biology of viruses. Academic Press, Inc., New York.
16. **Darnell, J. E., L. Levintow, M. M. Thoren, and J. L. Hooper.** 1961. The time course of synthesis of poliovirus RNA. Virology **13:**271–279.
17. **Dasgupta, A.** 1983. Purification of host factor required for *in vitro* transcription of poliovirus RNA. Virology **127:**245–251.
18. **Dasgupta, A., P. Zabel, and D. Baltimore.** 1980. Dependence of the activity of the poliovirus replicase on a host cell protein. Cell **19:**423–429.
19. **Dewalt, P. G.** 1990. Personal communication.
20. **Duechler, M., T. Skern, W. Sommergruber, C. Neubauer, P. Gruendler, I. Fogy, D. Blaas, and E. Kuechler.** 1987. Evolutionary relationships within the human rhinovirus genus: comparison of serotypes 89, 2, and 14. Proc. Natl. Acad. Sci. USA **84:**2605–2609.
21. **Fields, B. N., D. M. Knipe, R. M. Chanock, J. L. Melnick, B. Roizman, and R. E. Shope (ed.).** 1985. Virology. Raven Press, New York.
22. **Flanegan, J. B., and D. Baltimore.** 1977. Poliovirus-specific primer-dependent RNA polymerase able to copy poly(A). Proc. Natl. Acad. Sci. USA **74:**3677–3680.
23. **Giachetti, C., and B. L. Semler.** 1991. Role of a viral membrane polypeptide in strand-specific initiation of poliovirus RNA synthesis. J. Virol. **65:**2647–2654.
24. **Harris, K. S., W. Xiang, L. Alexander, W. S. Lane, A. V. Paul, and E. Wimmer.** 1994. Interaction of poliovirus polypeptide 3CD^{pro} with the 5′ and 3′ termini of the poliovirus genome: identification of viral and cellular cofactors needed for efficient binding. J. Biol. Chem. **269:**27004–27014.
25. **Hayes, R. J., and K. W. Buck.** 1990. Complete replication of a eukaryotic virus RNA *in vitro* by a purified RNA-dependent RNA polymerase. Cell **63:**363–368.
26. **Hey, T. D., O. C. Richards, and E. Ehrenfeld.** 1986. Synthesis of plus- and minus-strand RNA from poliovirion RNA template in vitro. J. Virol. **58:**790–796.
27. **Higgins, D. G., A. J. Bleasby, and R. Fuchs.** 1992. Clustal V: improved software for multiple sequence alignment. Comput. Appl. Biosci. **8:**189–191.
28. **Hughes, P. J., C. North, C. H. Jellis, P. D. Minor, and G. Stanway.** 1988. The nucleotide sequence of human rhinovirus 1B: molecular relationships within the rhinovirus genus. J. Gen. Virol. **69:**49–58.
29. **Imai, Y., Y. Matsushima, T. Sugimura, and M. Terada.** 1991. A simple and rapid method for generating a deletion by PCR. Nucleic Acids Res. **19:**2785.
30. **Jacobson, S. J., D. A. M. Konings, and P. Sarnow.** 1993. Biochemical and genetic evidence for a pseudoknot structure at the 3′ terminus of poliovirus RNA and its role in viral RNA amplification. J. Virol. **67:**2961–2971.
31. **Mizutani, S., and R. J. Colonno.** 1985. In vitro synthesis of an infectious RNA from cDNA clones of human rhinovirus 14. J. Virol. **56:**628–632.
32. **Molla, A., A. V. Paul, and E. Wimmer.** 1991. Cell-free *de novo* synthesis of poliovirus. Science **254:**1647–1651.
33. **Mosser, A. G., L. A. Caliguiri, and A. S. Scheid.** 1972. Chemical and enzymatic characteristics of cytoplasmic membranes of poliovirus-infected HeLa cells. Virology **47:**30–38.
34. **Noble, J., and L. Levintow.** 1970. Dynamics of poliovirus-specific RNA synthesis and the effects of inhibitors of virus replication. Virology **40:**634–642.
35. **Pardigon, N., and J. H. Strauss.** 1992. Cellular proteins bind to the 3′ end of Sindbis virus minus-strand RNA. J. Virol. **66:**1007–1015.
36. **Parekh, B., and G. W. Hatfield.** Ribosome release influences the basal level of transcription termination at the attenuator of the *ilv*GMEDA operon. Submitted for publication.
37. **Pilipenko, E. V., S. A. Maslova, A. N. Sinyakov, and V. I. Agol.** 1992. Towards identification of *cis*-acting elements involved in the replication of enterovirus and rhinovirus RNAs: a proposal for the existence of tRNA-like terminal structures. Nucleic Acids Res. **20:**1739–1745.
38. **Quadt, R., C. C. Kao, K. S. Browning, R. P. Hershberger, and P. Ahlquist.** 1993. Characterization of a host protein associated with brome mosaic virus RNA-dependent RNA polymerase. Proc. Natl. Acad. Sci. USA **90:**1498–1502.
39. **Richards, O. C., and E. Ehrenfeld.** 1990. Poliovirus RNA replication. Curr. Top. Microbiol. Immunol. **161:**89–119.
40. **Roehl, H. H., and B. L. Semler.** 1994. *In vitro* biochemical methods for investigating RNA-protein interactions in picornaviruses. Methods Mol. Genet. **4:**169–182.
41. **Roehl, H. H., and B. L. Semler.** 1995. Poliovirus infection enhances the formation of two ribonucleoprotein complexes at the 3′ end of viral negative-strand RNA. J. Virol. **69:**2954–2961.
42. **Sarnow, P., H. S. Bernstein, and D. Baltimore.** 1986. A poliovirus temperature-sensitive mutant located in a non-coding region of the genome. Proc. Natl. Acad. Sci. USA **83:**571–575.
43. **Semler, B. L., V. H. Johnson, P. G. Dewalt, and M. F. Ypma-Wong.** 1987. Site-specific mutagenesis of cDNA clones expressing a poliovirus proteinase. J. Cell. Biochem. **33:**39–51.
44. **Skern, T., W. Sommergruber, D. Blaas, P. Gruendler, F. Fraundorfer, C. Pieler, I. Fogy, and E. Kuechler.** 1985. Human rhinovirus 2: complete nucleotide sequence and proteolytic processing signals in the capsid protein region. Nucleic Acids Res. **13:**2111–2126.
45. **Tershak, D. R.** 1984. Association of poliovirus proteins with the endoplasmic reticulum. J. Virol. **52:**777–783.
46. **Towner, J. S., and B. L. Semler.** 1994. Unpublished results.
47. **Zuker, M., and P. Stiegler.** 1981. Optimal computer folding of large RNA sequences using thermodynamics and auxiliary information. Nucleic Acids Res. **9:**133–148.